

## LINEAR ELASTIC AND ELASTO-PLASTIC ASPECTS OF INTERFACE FRACTURE MECHANICS LINEARNO ELASTIČNI I ELASTOPLASTIČNI ASPEKTI MEHANIKE LOMA INTERFEJSA

Originalni naučni rad / Original scientific paper  
UDK /UDC:

Rad primljen / Paper received: 25.11.2020

Adresa autora / Author's address:

<sup>1</sup>Tel Aviv University, Dreszer Fracture Mechanics Laboratory, School of Mechanical Engineering, Ramat Aviv, Israel  
<sup>2</sup>University of Belgrade, Faculty of Mechanical Engineering, Belgrade, Serbia email: [asedmak@mas.bg.ac.rs](mailto:asedmak@mas.bg.ac.rs)

### Keywords

- interface fracture mechanics
- bi-material body
- J-integral
- singular finite element

### Abstract

This paper is written on the occasion of J.R. Rice's 80<sup>th</sup> birthday. Basically, it presents two aspects of interface fracture mechanics, linear elastic and elasto-plastic, both of them reflecting the long experience of the two authors. Special attention has been focused on the seminal contribution of Jim Rice, still being a great inspiration to researchers in the field of fracture mechanics. Fundamentals that he developed enabled us to build versatile scientific and engineering tools that currently enable the solution of almost any problem related to cracks.

### INTRODUCTION

Before discussing linear elastic interface fracture mechanics, let us recall the initiation of fracture mechanics. In 1921, Griffith /1/ wrote his ground breaking paper on fracture mechanics in which he showed that the stresses in brittle material near a crack tip depend on the inverse square-root of the crack length. He estimated the theoretical strength of glass. Moreover, he presented his energetic criterion for crack propagation. The next major step took place after World War II with the development of the first term of the asymptotic expansion for the stresses and displacements in the neighbourhood of a crack tip in a linear elastic, homogeneous and isotropic material /2, 3/. Modes of deformation, as well as the definition of the stress intensity factors,  $K_I$ ,  $K_{II}$  and  $K_{III}$  may be found in /4/.

### LINEAR ELASTIC INTERFACE FRACTURE

The first paper on interface fracture mechanics appears shortly after /5/. The behaviour of the stresses and displacements in the neighborhood of a crack tip for a crack along an interface between two dissimilar linear elastic, isotropic and homogeneous materials is found (see Fig. 1). It is seen that the stresses exhibit a square-root, oscillatory singularity at the crack tip. That is, the stresses oscillate ever faster while approaching infinity in a square-root sense as the crack tip is approached. It was shown that the oscillations occur very close to the crack tip. It was not noted, but it is predicted that the crack faces in the neighborhood of the crack tip interpenetrate which is not physically tenable.

### Ključne reči

- mehanika loma interfejsa
- bimaterijalno telo
- J-integral
- singularni konačni element

### Izvod

Ovaj rad je napisan povodom 80-tog rođendana J.R. Rajsa. U njemu su suštinski predstavljena dva aspekta mehanike loma interfejsa - linearno elastični i elasto-plastični, u kojima se odražava dugogodišnje iskustvo oba autora. Posebna pažnja je posvećena ključnim doprinosima Džima Rajsa, koji i dan-danas inspirišu istraživače koji rade na polju mehanike loma. Osnove koje je on razvio su dale temelj za igradnju naučnih i inženjerskih alata koji trenutno omogućavaju rešavanje skoro svih problema vezanih za prslinae.

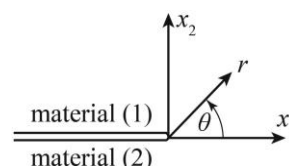


Figure 1. Crack tip coordinates

Nonetheless, this work was followed by a series of papers. In /6/, the problem of an infinite body with several interface cracks and applied far field point loads was considered. The first term of the asymptotic expansion for the stresses was determined, as well as the stress intensity factors for two specific geometries. The oscillatory parameter was found as

$$\varepsilon = \frac{1}{2\pi} \ln \left( \frac{\kappa_1 \mu_2 + \mu_1}{\kappa_2 \mu_1 + \mu_2} \right), \quad (1)$$

where:

$$\kappa_k = \begin{cases} 3-4\nu_k & \text{plane strain} \\ \frac{3-\nu_k}{1+\nu_k} & \text{generalized plane strain} \end{cases} \quad (2)$$

$\kappa_k$  are the shear moduli; and  $\nu_k$  are the Poisson's ratios of the upper  $k = 1$ , and lower materials  $k = 2$ , respectively. It is also pointed out in /6/ that the oscillatory stresses are relegated to a very small region ahead of the crack tip. In /7/, the problem of an interface crack between two dissimilar plates was considered by Sih and Rice. Again, a square-root, oscillatory singularity was found for the stresses. Here, as well, the asymptotic expansion for the stresses is found. In an appendix, following up in /5, 6/, the first term

of the asymptotic expansion of the stresses is found for the in-plane problem. The in-plane problem is reconsidered by Rice and Sih /8/. Three problems are solved using the Kolosov-Muskhelishvili method to determine the Gourset functions. One is a semi-infinite interface crack subjected to point loads; the second is a finite length interface crack in an infinite body shown in Fig. 2; and the third is a periodic array of finite length interface cracks in an infinite body. Stress intensity factors  $k_1$  and  $k_2$  were found for each of the problems. Significantly, it was noted that these stress intensity factors no longer represent modes I and II deformations. The deformation is now coupled. In an appendix, for the infinite body shown in Fig. 2, it is found that horizontal stresses must be applied for  $|x_1| \rightarrow \infty$ , so that the displacements will be continuous across the interface. The normal stress in the lower material  $\sigma_{11}^{(2)}$  is found as

$$\sigma_{11}^{(2)} = \frac{\bar{E}_2}{\bar{E}_1} \sigma_{11}^{(1)} + \left[ \frac{3 - \kappa_2}{1 + \kappa_2} - \frac{3 - \kappa_1}{1 + \kappa_1} \frac{\bar{E}_2}{\bar{E}_1} \right] \sigma_{22}^{\infty}, \quad (3)$$

where the normal stress in material 1,  $\sigma_{11}^{(1)}$ , is chosen arbitrarily; and  $x_2$  is the far field applied stress in the - direction; the Young's moduli are defined as

$$\bar{E}_k = \begin{cases} \frac{E_k}{1 - \nu_k^2} & \text{plane strain} \\ E_k & \text{generalized plane strain} \end{cases} \quad (4)$$

where:  $k = 1, 2$  represents the upper and lower materials, respectively; and  $E_k$  are the Young's moduli of the upper and lower materials, respectively.

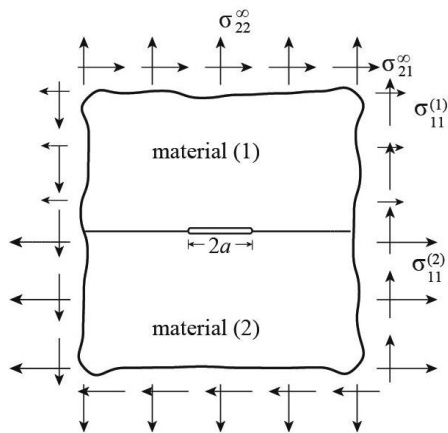


Figure 2. Infinite bimaterial body with a finite length crack, subjected to remote tension and shear.

In /9/, a problem was solved of a crack of finite length  $2a$  along an interface between two half-spaces of dissimilar material shown in Fig. 2, where the crack was subjected to constant opening pressure. It was found again that the stress oscillations were confined to a small distance from the crack tip. Moreover, it was shown that there is crack face interpenetration also confined to a small region which was estimated to be a maximum of  $0(10^{-4})$  of the crack length  $2a$ . It was noted that this is sufficiently small and may be neglected so that the solution to such problems may be considered as a good approximation to the physical problem. The effect of shear loading was mentioned in passing to also have small interpenetration zones. This will be seen not

to be the case. Several different interface crack problems are considered in /10/. Again it is shown for applied tensile loading that the stress oscillations begin very close to the crack tip. Moreover, for an interface crack between glass and steel with tensile loading, crack face interpenetration begins at a distance of  $10^{-7}a$ , where  $a$  is the half crack length.

Again it was shown in /11/ that oscillations of the stresses on the interface ahead of the crack tip are in a small region and the interpenetration of the crack face is also in a small region. All authors that have addressed this issue have not considered the application of shear stresses. In that paper, it was pointed out, that instead of interpenetration, a contact zone would occur. The authors also bring to our attention a paper by Cherepanov /12/ published in 1962 in Russian, where the Gourset functions were determined showing the oscillatory behaviour. For the first time, the interface energy release rate is related to the stress intensity factors by /11/:

$$\mathcal{G}_i = \frac{\pi}{4 \cosh^2 \pi \varepsilon} \left( \frac{1}{\bar{E}_1} + \frac{1}{\bar{E}_2} \right) (A_0^2 + B_0^2), \quad (5)$$

where:  $\varepsilon$  is given in Eq.(1);  $\bar{E}_k$  is given in Eq.(4); and  $A_0$  and  $B_0$  are the modes 1 and 2 stress intensity factors, in respect. These stress intensity factors differ by a factor from  $k_1$  and  $k_2$  given in /8/.

It would appear that as a result of the oscillations of the stresses in the neighborhood of the crack tip and the interpenetration of the crack faces that interest was lost in exploring the behaviour of interface cracks. In 1971, two papers appeared in which a crack in an interlayer between two semi-infinite half-planes was investigated /13, 14/. The first finite element solution for an interface crack was presented in 1976 /15/ using a special crack tip element and a hybrid method. The stress oscillations were mentioned, but crack face interpenetration was not.

Next, Comninou took another approach in a series of three papers /16-18/. In /16/, the bimaterial problem of an infinite body containing a finite length crack along the interface shown in Fig. 2 and subjected to far field tension was considered. It was assumed that two contact zones exist at each end of the crack. The length of the contact zones were found as part of the solution to the problem to be between  $10^{-7}a$  and  $10^{-4}a$ , where  $a$  is the half-crack length. The contact zone was shown to be smaller than the interpenetration zone. For pure applied far field shear stresses /17/, it was seen that the contact zone on one side of the crack was smaller than that for applied tension, whereas the contact zone on the other side of the crack was approximately two-thirds of the half-crack length. The side at which the large contact zone occurs depends on the mechanical properties of the materials on either side of the interface, as well as the direction of the shear stress. The small contact zone is larger than the interpenetration zone. In /18/, combined applied tension-compression and shear stresses were considered. Interestingly, when compression is applied, part of the crack remains open.

Use of the approach developed by Comninou for other geometries would be difficult. Instead, in 1988, Rice /19/ returns to the problem of an interface crack giving guidance on how the problem should be approached, allowing for

zones of crack face interpenetration. In that paper, methods of Muskhelishvili are used to obtain the potential functions for the interface crack. The tractions along the interface were found to be:

$$(\sigma_{22} + i\sigma_{21})|_{\theta=0} = \frac{K r^{i\varepsilon}}{\sqrt{2\pi r}}, \quad (6)$$

where:  $i = \sqrt{-1}$ ; the crack tip polar coordinates  $r$  and  $\theta$  are illustrated in Fig. 1; the complex stress intensity factor may be written as:

$$K = K_1 + iK_2, \quad (7)$$

where:  $K_1$  and  $K_2$  are real and are the modes 1 and 2 stress intensity factors; and the oscillatory parameter  $\varepsilon$  is given in Eq.(1). It may be noted that in /19/, the subscripts I and II are used instead of 1 and 2. Below, this choice will be elaborated. Moreover, the complex stress intensity factor defined in /7, 8/ is related to that in Eq.(7) by:

$$K = \sqrt{\pi} \cosh \pi \varepsilon (k_1 + ik_2), \quad (8)$$

and those defined in Eq.(5) are related as

$$K = \sqrt{\frac{\pi}{2}} (A_0 + iB_0). \quad (9)$$

Along the crack faces

$$\Delta u_2 + i\Delta u_1 = \frac{4}{(1 + 2i\varepsilon) \cosh \pi \varepsilon} \left( \frac{1}{E_1} + \frac{1}{E_2} \right) \sqrt{\frac{r}{2\pi}} K r^{i\varepsilon}, \quad (10)$$

where

$$\Delta u_i = u_i^{(1)}(r, \pi) - u_i^{(2)}(r, -\pi), \quad (11)$$

the subscript  $i = 1, 2$  represents the coordinate directions in Fig. 1; and the superscript  $k = 1, 2$  represents the upper and lower materials, respectively. Using Eqs.(6) and (10) in the Irwin crack closure integral /3, 4/, the interface energy release rate is found as:

$$\mathcal{G}_i = \frac{1}{2 \cosh^2 \pi \varepsilon} \left( \frac{1}{E_1} + \frac{1}{E_2} \right) (K_1^2 + K_2^2), \quad (12)$$

where: the subscript  $i$  represents interface.

Substituting Eq.(9) into Eq.(12) reproduces Eq.(5).

As an example, the stress intensity factor for a finite length interface crack between two semi-infinite half-spaces subjected to far field uniform tension  $\sigma_{22}^\infty$  and shear  $\sigma_{21}^\infty$  stresses, as shown in Fig. 2, is given by:

$$K = (\sigma_{22}^\infty + i\sigma_{21}^\infty) (1 + 2i\varepsilon) \sqrt{\pi a} (2a)^{-i\varepsilon}. \quad (13)$$

Note that the far field normal stress in the  $x_1$  direction in Eq.(3) is applied.

Rice goes on in /19/ to elucidate the validity of the first term of the asymptotic expansion for the stresses and displacements by the argument that if the region of crack face interpenetration is sufficiently small as to be enclosed in a small scale nonlinear zone, the  $K$  solution is valid in an annular region outside this zone and governs the behaviour of the crack. To this end, this region was estimated by determining the value of  $r$  for which  $\Delta u_2 = 0$ . The applied far field stress for the problem shown in Fig. 2 may be written as

$$\sigma_{22}^\infty + i\sigma_{21}^\infty = T e^{i\psi} \quad (14)$$

where:  $T$  is the magnitude of the traction vector; and the phase angle  $\psi$  gives its direction. Setting  $\Delta u_2 = 0$  in Eq.(10), leads to:

$$r_c = 2a \exp \left[ -\frac{1}{\varepsilon} \left( \psi + \frac{\pi}{2} \right) \right], \quad (15)$$

for the radius in which there is  $K$  - dominance for  $\varepsilon > 0$ . If  $\varepsilon < 0$  the labels for the upper and lower materials are exchanged and  $\psi$  is replaced by  $-\psi$ . Since  $\varepsilon \ll 1$ ,  $r_c/2a$  is much smaller than unity, at least for  $-\pi/4 < \psi < \pi/2$ .

In general,  $\varepsilon$  increases with the ratio  $\mu_2/\mu_1$ . As an example, taking material 1 as cork with  $\nu_1 \approx 0$  and bonding it to a stiff material so that  $\mu_1/\mu_2 \approx 0$ , then the largest value of  $\varepsilon$  in Eq.(1) is 0.175. Example values of  $\varepsilon$  are given: for SiO<sub>2</sub> as the upper material and Al<sub>2</sub>O<sub>3</sub> as lower material  $\varepsilon = 0.075$ ; for Si and Cu as upper and lower materials,  $\varepsilon = 0.011$ . Other examples are given in /19/.

If one wishes to duplicate the crack tip conditions for two bodies with different crack lengths, one must apply different loading conditions to each body. If the crack length is  $2a$  in one body shown in Fig. 2, and  $\psi = 0$  in Eq.(14) so that only tensile loading is applied, then a crack of length  $2a'$  requires a combination of tensile and shear loading to obtain the same  $K$  field. This means that it is not possible to separate opening and in-plane sliding modes. This is different from cracks in homogeneous materials where the modes I and II stress intensity factors are written as  $K_I$  and  $K_{II}$ , representing opening and in-plane sliding deformation.

It is shown that if the crack length is changed from  $2a$  to  $2a'$  for the problem in Fig. 2, the traction in eq. (14) must be changed as:

$$T' = T \sqrt{\frac{a}{a'}}, \quad (16)$$

as is the case for homogeneous material. But the phase angle of the loading must also be altered as:

$$\psi' = \psi + \varepsilon \ln \left( \frac{a'}{a} \right). \quad (17)$$

Thus, the ratio between the stress intensity factor changes which does not occur in homogeneous material where the ratio of  $K_I$  and  $K_{II}$  remains fixed. The phase angle change  $\psi' - \psi$  is generally small since  $\varepsilon$  is small. For  $\varepsilon = 0.175$ , its maximum value, and  $a'/a = 100$ ,  $\psi' - \psi = 46^\circ$ . However, for  $\varepsilon = 0.011$ , for Si/Cu,  $\psi' - \psi = 2.9^\circ$ .

The unit of the complex stress intensity factor in meters is

$$\text{MPa}\sqrt{\text{m}}(\text{m})^{-i\varepsilon}. \quad (18)$$

Changing from meters to millimetres changes the ratio of the stress intensity factors  $K_2/K_1$ . Thus, opening and sliding deformation of the crack are inherently coupled. Applied loads cannot be unambiguously connected with mode I and mode II deformation.

It was suggested to normalize the units of the complex stress intensity factor by multiplying it by some length parameter raised to the power  $i\varepsilon$ , that is:

$$\hat{K} = \hat{K}_I + i\hat{K}_{II} = K \hat{L}^{i\varepsilon}, \quad (19)$$

where  $K$  is given in Eq.(7). The length parameter  $\hat{L}$  remains to be defined. But in Eq.(19), the stress intensity factor  $\hat{K}$  has the usual units of stress intensity factors. It was suggested as a possibility to choose  $\hat{L}$  as a characteristic length of the fracture process zone in a specific test. This parameter should be a constant and not related to a changing crack length. It may be noted that one of the authors has used  $\hat{L}$  to correlate failure data and a failure curve; see reference /20/ as an example.

For small scale yielding in which one or both solids deform plastically, the dimensions of the plastic zone depends on the complex stress intensity factor  $K$  and material properties. These properties depend on the yield stress  $\sigma_0$  of the weaker solid, the ratio of the yield stresses and dimensionless properties describing strain hardening and ratios of elastic constants. See /19/ for a dimensional analysis of the plastic zone size.

An additional square-root singularity was found and discussed in /19, 21/. In /21/, the in-plane stresses were written as:

$$\sigma_{\alpha\beta} = \frac{1}{\sqrt{2\pi r}} \left[ \Re(Kr^{i\varepsilon}) \Sigma_{\alpha\beta}^{(1)}(\theta, \varepsilon) + \Im(Kr^{i\varepsilon}) \Sigma_{\alpha\beta}^{(2)}(\theta, \varepsilon) \right], \quad (20)$$

where:  $\alpha, \beta = 1, 2$ ;  $\Re$  and  $\Im$  represent the real and imaginary parts of the quantity in parenthesis;  $K$  is the complex stress intensity factor in Eq.(7);  $r$  and  $\theta$  are the crack tip polar coordinates shown in Fig. 1; and  $\Sigma_{\alpha\beta}^{(j)}$ , where  $j = 1, 2$ , is a well behaved function of the oscillatory parameter  $\varepsilon$  and the crack tip polar coordinate  $\theta$ . In addition, for out-of-plane deformation

$$\sigma_{3\beta} = \frac{K_{III}}{\sqrt{2\pi r}} \Sigma_{3\beta}^{(III)}(\theta), \quad (21)$$

where:  $K_{III}$  is the mode III stress intensity factor which is the amplitude of a square-root singularity. The existence of a square-root singularity was mentioned in /19/. The functions  $\Sigma_{\alpha\beta}^{(j)}$ ,  $j = 1, 2$ , are presented in /21/ where the coordinate directions are in polar coordinates. The functions  $\Sigma_{\alpha\beta}^{(j)}$ ,  $j = 1, 2$ , and  $\Sigma_{\alpha\beta}^{(III)}$  are presented in /22/, where the coordinate directions are in Cartesian coordinates. Of course, these functions differ for the upper and lower materials.

The phase angle in Eq.(17) is redefined in /21/ as the phase angle of the stress intensity factor which may be written as:

$$\psi = \arctan \left[ \frac{\Im(KL^{i\varepsilon})}{\Re(KL^{i\varepsilon})} \right], \quad (22)$$

where:  $L$  is a length parameter. A change in the length parameter from  $L_A$  to  $L_B$  translates the value of the phase angle as:

$$\psi_A = \psi_B + \varepsilon \ln \left( \frac{L_A}{L_B} \right). \quad (23)$$

The problem of an interface crack between two dissimilar anisotropic materials was also discussed in /21/. It was pointed out that it is possible that the square-root, oscillatory singularity is related to the in-plane deformation as shown in Eq.(7) and that the out-of-plane deformation is related to the square-root singularity. But it is also possible that the shear deformation, both in-plane and out-of-plane are coupled with a complex stress intensity factor given by:

$$K = K_2 + iK_3, \quad (24)$$

being the amplitude of the square-root, oscillatory singularity, and  $K_1$  being the amplitude of the square-root singularity. In fact, it has been shown /23/ that there can be three stress intensity factors which are the amplitude of the square-root singularity and three stress intensity factors related to the square-root, oscillatory singularity.

A failure criterion was proposed based on  $\mathcal{G}_c$  as a function of the phase angle  $\psi$  for a given value of  $L$ . This failure criterion is a fracture toughness locus of the interface where the subscript  $c$  denotes critical. That paper goes on to discuss the competition between interface cleavage and dislocation emission.

Finally, with papers /19/ and /21/, Rice's contribution was seminal to the reinvigoration of the subject of interface fracture mechanics which motivated the publication of hundreds of papers on the subject.

#### ELASTO-PLASTIC INTERFACE FRACTURE MECHANICS

The J-integral has been used extensively as a fracture mechanics parameter for more than 50 years, ever since it was defined by Rice in 1968, /24/, as a conservation law for a two-dimensional (2D) cracked body. It was proved by Rice /24/ that the J-integral is path independent, it can be identified with crack driving force, and it describes the stress and strain fields around crack /25, 26/. As stated in the Rice's original paper, the J-integral is valid for two-dimensional plane (nonlinear) elasticity in the absence of body and thermal forces, and for the homogeneous material, at least in crack direction. Of course, there are no tractions on the crack faces. Its application beyond these limitations has been questionable, but still successful, e.g. for elasto-plastic fracture mechanics without any modifications of the original expression /27/. In some other cases, modified J-integrals were introduced to compensate for missing path independence, e.g. for elasto-dynamics, /28/ and for a 2D curved body, /29-31/. Besides the original paper by Rice /24/, several later contributions should be mentioned /32-34/.

Here, one of the limitations of the original definition of J-integral is expanded upon and described here in more detail. It has been the focus of the second author for more than 30 years /35-37/. It is the problem of weldment heterogeneity, represented as a multibody with interfaces between regions with different properties /35-39/. As follows from the original definition, the J-integral is not path independent for a generally shaped weldment. But its path independence may be recovered if a modified J-integral is introduced, comprising the original J-integral and line integrals along weldment interfaces /38-39/. Towards this end, we present here the modified J-integral for a multi-material body, representing a welded joint with four different material regions (base metal - BM, weld metal - WM, coarse grain heat affected zone - CGHAZ and fine grain heat affected zone - FGHAZ), including the results presented in /35-37/.

The modified J-integral for a weldment

The modified J-integral for a weldment will be introduced as for a multi-material body, represented by four regions of different material properties as shown in Fig. 3: BM, WM and two regions in HAZ - one with fine grained structure (FG) and the other one with coarse grained structure (CG). Such a representation follows the uneven strain distribution along a weldment, with two extremes in HAZ, as shown in /35-37/. This is also in accordance with the well-known structural heterogeneity of HAZ: fine grain normalized region and coarse grain overheated region.

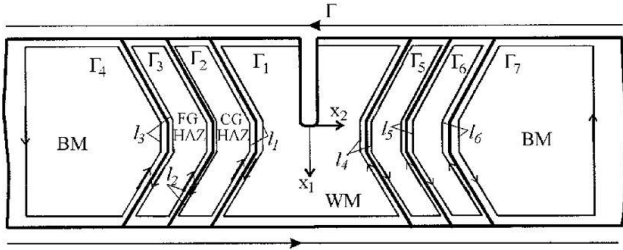


Figure 3. Integration paths for weldment, /35/.

The J-integral may be evaluated along a path  $\Gamma_1$  encompassing the crack and not crossing the interface:

$$J_{\Gamma_1} = \int_{\Gamma_1} \left( Wn_1 - \sigma^{ij}n_j \frac{\partial u^i}{\partial x^1} \right) ds = G, \quad (25)$$

where:  $W$  denotes the strain energy density;  $n_j$  is the unit outward normal to  $\Gamma_1$ ;  $\sigma^{ij}$  is the stress tensor;  $u^i$  is the displacement vector;  $x^1$  are Cartesian coordinates ( $x^1$  is along crack); and  $G$  is the energy release rate or crack driving force. For six closed paths,  $\Gamma_2$ - $\Gamma_7$  as shown in Fig. 3, the crack driving force  $G = 0$ , so that

$$\int_{\Gamma_a} \left( Wn_1 - \sigma^{ij}n_j \frac{\partial u^i}{\partial x^1} \right) ds = 0, \quad a = 2, 3, 4, 5, 6, 7. \quad (26)$$

The J-integral along paths  $\Gamma_2$ - $\Gamma_7$  reduces to zero because these paths do not encompass any discontinuities. Using Eqs.(25) and (26) one can write:

$$J = \int_{\Gamma} \left( Wn_1 - \sigma^{ij}n_j \frac{\partial u^i}{\partial x^1} \right) ds - \sum_{a=1}^6 \int_{l_a} \left( Wn_1 - \sigma^{ij}n_j \frac{\partial u^i}{\partial x^1} \right) ds, \quad (27)$$

where:  $l_a$ ,  $a = 1 \dots 6$ , denote the closed contour along material interfaces. All of the paths along the interfaces,  $l_a$ , comprise parts of  $\Gamma_a$ ,  $a = 2 \dots 7$ , e.g.,  $l_3$ , comprises those parts of  $\Gamma_3$  and  $\Gamma_4$ , which are along the interface between BM and FG HAZ, Fig. 3. Once all pieces are put together, the expression in Eq.(27) follows, defining the modified J-integral for a weldment, represented by four regions with different material properties. The modified J-integral is path independent, as shown in /35-37/. It has the following physical meaning: the first integral represents the force acting on both the crack tip and material interfaces (discontinuities of stress and strain), whereas the second one eliminates the force on the boundaries. Thus, the complete integral expression represents only the force acting on the crack tip, and can be identified with the energy release rate due to a unit crack growth.

Numerical procedure - historical retrospective and application

Numerical analysis of elasto-plastic material behaviour is performed using collapsed isoparametric eight-noded elements around the crack tip, producing a  $r^{-1}$  singularity. It should be noted that singular elements are one of three important contributions of JRR (this list is not complete, but just focused on topics covered here), the other two being the J-integral itself and the HRR fields /24-27/ as described in /40/. Therefore, it is natural to quote here several statements from the brilliant paper, written by Rice and Tracey in the early seventies /41/. (Note: original reference numbers are retained in parentheses and these papers are referenced here in the next paragraph, using different numbers): ‘Three types of finite elements were used in the analysis. For elastic solutions the  $r^{-1/2}$  singular element (ref. 25) was used nearest the crack tip with arbitrary quadrilateral 4-noded isoparametric elements over the remainder of the configuration. To study plastic effects at the crack tip, a new singular element was designed, similar to that of Levy et al. (ref 37), which has a  $1/r$  shear strain singularity (with a bounded dilatational strain) and a uniform strain as admissible deformations. The singular elements have the shape of isosceles triangles and are focused along radial lines at the crack tip. However, they are treated as degenerate isosceles trapezoids in the sense that four nodes are assigned to the elements, one at each vertex, even though two of the nodes coincide at the crack tip. Levy et al. (37) introduced this coincident node technique to study the crack tip displacement variation. Contrary to their procedure, however, the coincident nodes were here constrained to move as a single point in obtaining the elastic response of the cracked body, since the non-unique crack tip displacement is a plasticity effect. The variation of stress and hence the constitutive relation in the plastic case within elements was accounted for in the following approximate manner. Each near-tip element was viewed as the composite of three sub-elements, each extending one-third of the height of the element. The area average strain of an individual sub-element was used in evaluating the stress state and constitutive matrix representative of the sub-element. The three sub-element stiffnesses were then formed and added to obtain the total element stiffness matrix. For the adjoining isoparametric elements, the midpoint strain was judged adequate to calculate the stress representative of the entire element. To obtain elasto-plastic solutions, the procedure was to specify the  $r^{-1/2}$  element just up to the load necessary to yield one of the sub-elements. Thereupon, the  $r^{-1}$  element was used with its associated nonunique crack tip displacement capability. Clearly, the elastic singularity implies yielding under infinitesimal load so that there is some error involved in the plastic solution by specifying the  $r^{-1/2}$  near tip strain distribution up to finite loads. Actually, for the element size used at the tip, this error should be very small.’

Let us keep in mind the fact that all necessary equations for both linear elastic and elasto-plastic elements were provided, including relevant examples, in /41-43/, establishing a computational fracture mechanics framework already in 1973. In addition, let us recall that just two years later, McMeeking and Rice (1975) /44/ have shown that triangular

or prismatic collapsed 8- or 20-noded elements, respectively, with a  $1/r$  singularity, are well suited for elasto-plastic 2D and 3D calculations, also used here. Having in mind also the pioneering work in the mechanics of crack tip deformation and extension by fatigue /45/, it seems that we are still just recycling efforts and results provided by James Rice in the late sixties and early seventies.

Results

In order to check the influence of weldment heterogeneity on the J-integral value obtained by direct measurement on the surface of a cracked tensile panel, its cross-section through the maximum crack depth was analysed by the finite element method, using a mesh consisting of 297 8-noded elements and 822 nodes, including singular elements at the crack tip, as shown in Fig. 5a. Both integral terms in Eq.(27) were numerically evaluated on different paths ( $J_1$ - $J_3$ ) shown in Fig. 5. All other data is given in /35-37/, including mechanical properties (yield stress  $R_{eh}$  and hardening coefficient  $H'$ ) of weldment regions, which are used for bi-material representation of stress-strain curves.

The results are given in Table 1, showing the average value of the J-integral for six inner paths,  $J_{AVE}$ , close to the crack tip and not intersecting material boundaries (each two paths crossing three rings of elements around the crack tip, paths 1 & 2 – elements 8, 9, 12, 15, 18; paths 3 & 4 – elements 7, 10, 13, 16, 19; paths 5 & 6 – elements 6, 11, 14, 17, 20; in Fig. 5b), the values of first integral term in the modified J-integral for the remote paths intersecting the material boundaries ( $J_1$ ,  $J_2$  and outer path  $J_3$  in Fig. 5a), and the values of the second integral term in the modified J-integral along the boundaries between WM and CG HAZ ( $l_1$ ), between CG HAZ and FG HAZ ( $l_3$ ), and between FG HAZ and BM ( $l_3$ ).

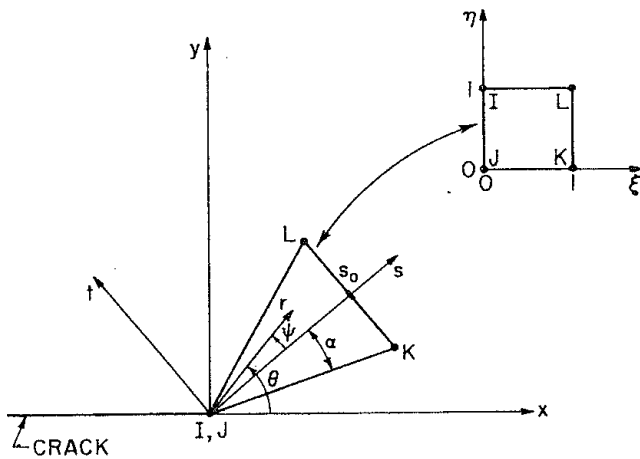


Figure 4. Singular crack tip element, as introduced in /42/.

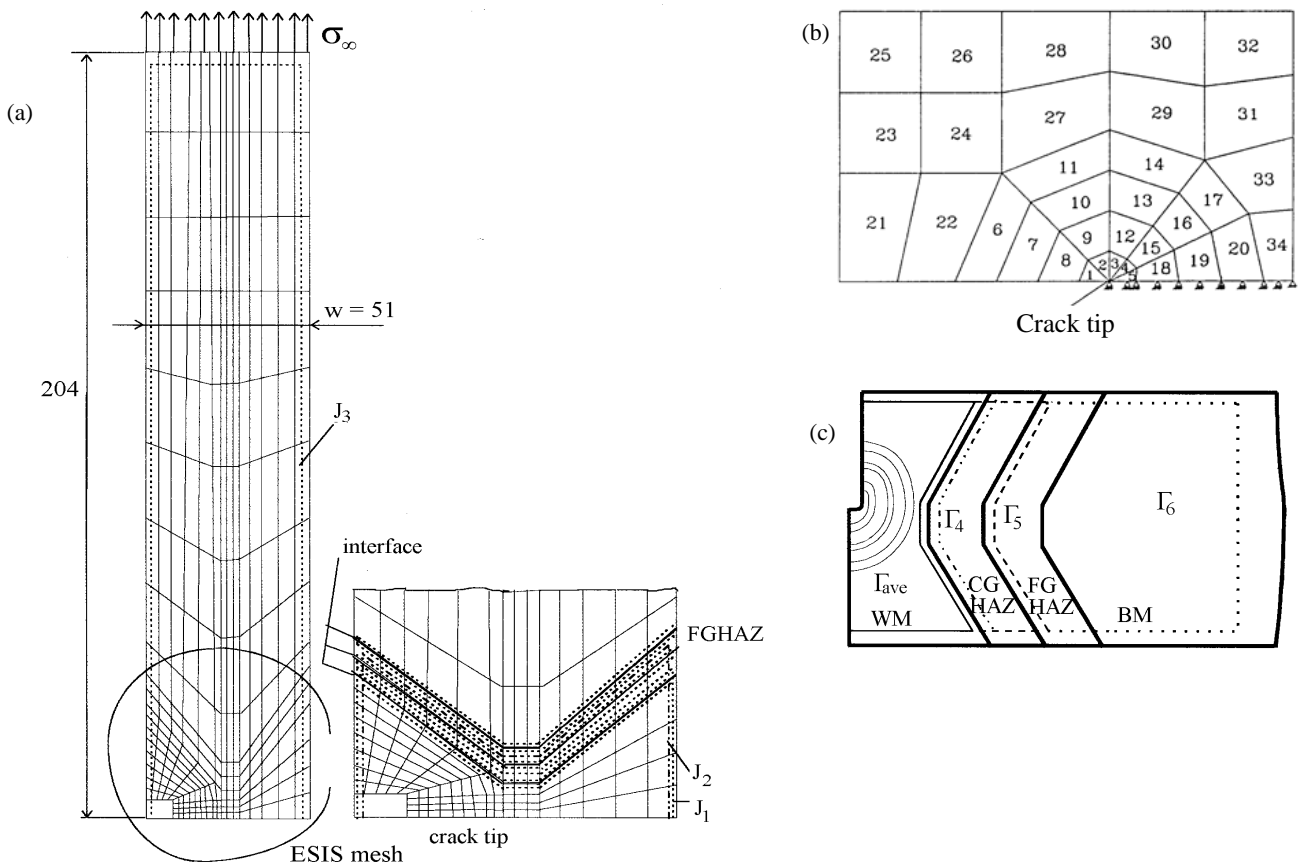


Figure 5. Finite element mesh: (a) with details around the crack tip: mesh (b) and weldment zones (c).

Table 1. Results for  $J_1$ - $J_6$  integrals (inner paths through the weld metal).

Remote load $\sigma_\infty$ (MPa)	$J_1$ (N/mm)	$J_2$ (N/mm)	$J_3$ (N/mm)	$l_1$ (N/mm)	$l_2$ (N/mm)	$l_3$ (N/mm)	$J_{AVE}$ (N/mm)
700	41.306	42.278	44.679	-0.790	0.341	-0.350	39.715
710	72.604	71.227	79.238	-2.998	2.661	-1.039	68.318
720	100.481	95.6042	106.957	-5.582	5.808	-4.167	92.567
730	133.131	124.831	139.410	-8.226	9.081	-7.270	122.440
740	160.795	149.400	166.615	-11.308	12.088	-10.070	148.362
750	202.666	187.190	206.002	-16.322	16.497	-14.327	188.772
760	223.504	205.236	225.386	-18.716	19.324	-17.222	209.220
770	247.370	225.526	247.658	-21.401	23.043	-20.973	232.632

As may be seen in Table 1, the finite element results confirm the theoretical analysis of the material interface effect on the J-integral value. Namely, the Rice's J-integral is path dependent because its values for different paths differs only by the limits of numerical error. The largest difference ( $J_1$  and  $J_2$ ) is cca 9%, while the numerical error may be estimated to cca 2.5%, /35/. On the other hand, if values of the modified J-integral (defined by Eq.(27) and denoted here as  $J_w$ ), shown in Table 2, are obtained, one may observe excellent agreement between  $J_{w1}$ ,  $J_{w2}$  and  $J_{w3}$ , as well as good agreement (within the limits of numerical error) between these values and  $J_{AVE}$ . The relations between  $J_1$ - $J_3$  and  $l_1$ - $l_3$  with  $J_{w1-3}$  is as follows:

$$J_{w1}=J_1+l_1, \quad (28)$$

$$J_{w2}=J_2+l_1+l_2, \quad (29)$$

$$J_{w3}=J_3+l_1+l_2+l_3. \quad (30)$$

Table 2. Results for the modified J integral.

Remote load $\sigma_\infty$ (MPa)	$J_{AVE}$ (N/mm)	$J_{w1}$ (N/mm)	$J_{w2}$ (N/mm)	$J_{w3}$ (N/mm)
700	39.715	40.516	41.829	44.580
710	68.318	69.605	70.889	77.861
720	92.567	94.899	95.830	103.016
730	122.440	124.905	125.686	132.995
740	148.362	149.486	150.180	157.324
750	188.772	186.343	187.365	191.850
760	209.220	204.787	205.844	208.772
770	232.632	225.968	227.167	228.326

From an engineering standpoint, the effect of weldment heterogeneity is neither significant nor negligible. One can see that the J-integral that corresponds to the directly measured value (path  $J_3$ ) is almost cca 8% higher than the real one (247.658 vs. 228.326). Having in mind the shape of weldment and differences in properties, one can hardly imagine a more critical situation when similar materials are welded. Anyhow, dissimilar materials (e.g. ferrite and martensite or austenite steels) would produce much larger differences between the J-integral for the outer contour and the modified J-integral. This is especially important if a directly measured J-integral is used as the J-R curve for the undermatched dissimilar weldments, because large overestimation can be obtained /46-50/.

As a final note, it may be pointed out that the J-integral is more frequently calculated as an area integral which leads to more accurate results /51/. These analyses are further discussed in /52, 53/. More information on linear elastic fracture mechanics of interface cracks may be found in /54/.

Nonetheless, the line integrals were used because with area integrals path independency could have not been analysed in the way shown here.

## REFERENCES

- Griffith, A.A. (1921), *The phenomena of fracture and flow in solids*, Phil. Trans. R. Soc. A, 221(582-593): 163-198. doi: 10.1098/rsta.1921.0006
- Williams, M.L. (1956), *On the stress distribution at the base of a stationary crack*, J Appl. Mech. 24(1): 109-114.
- Irwin, G.R. (1957), *Analysis of stresses and strains near the end of a crack traversing a plate*, Trans. ASME, Ser. E, J Appl. Mech. 24: 361-364.
- Irwin, G.R. (1958), *Fracture*, In: *Elasticity and Plasticity*, S. Flügge (ed.), Series: Mechanical and Thermal Behaviour of Matter, Springer, Germany, pp.551-590.
- Williams, M.L. (1959), *The stresses around a fault or crack in dissimilar media*, Bull. Seismol. Soc. Am. 49(2): 199-204.
- Erdogan, F. (1963), *Stress distribution in a nonhomogeneous elastic plane*, J Appl. Mech., 30(2): 232-236. doi: 10.1115/1.3636517
- Sih, G.C., Rice, J.R. (1964), *The bending of plates of dissimilar materials with cracks*, J Appl. Mech. 31(3): 477-482. doi: 10.1115/1.3629665
- Rice, J.R., Sih, G.C. (1965), *Plane problems of cracks in dissimilar media*, J Appl. Mech. 32(2): 418-423. doi: 10.1115/1.3625816
- England, A.H. (1965), *A crack between dissimilar media*, J Appl. Mech. 32(2): 400-402. doi: 10.1115/1.3625813
- Erdogan, F. (1965), *Stress distribution in bonded dissimilar materials with cracks*, J Appl. Mech. 32(2): 403-410. doi: 10.1115/1.3625814
- Malyshev, B.M., Salganik, R.L. (1965), *The strength of adhesive joints using the theory of cracks*, Int. J Fract. Mech. 1: 114-128. doi: 10.1007/BF00186749
- Cherepanov, G.P. (1962), *The stress state in a heterogeneous plate with slits*, Izvestija AN SSSR, OTN, Mekhan. i Mash., 1: 131-137 (in Russian).
- Erdogan, F., Gupta, G. (1971), *The stress analysis of multi-layered composites with a flaw*, Int. J Solids Struct. 7(1): 39-61. doi: 10.1016/0020-7683(71)90017-5
- Erdogan, F., Gupta, G.D. (1971), *Layered composites with an interface flaw*, Int. J Solids Struct. 7(8): 1089-1107. doi: 10.1016/0020-7683(71)90082-5
- Lin, K.Y., Mar, J.W. (1976), *Finite element analysis of stress intensity factors for cracks at a bi-material interface*, Int. J. Fract. 12: 521-531. doi: 10.1007/BF00034638
- Comninou, M. (1977), *The interface crack*, J Appl. Mech. 44(4): 631-636. doi: 10.1115/1.3424148
- Comninou, M. (1978), *The interface crack in a shear field*, J Appl. Mech. 45(2): 287-290. doi: 10.1115/1.3424289



18. Comninou, M., Schmueser, D. (1979), *The interface crack in a combined tension-compression and shear field*, J Appl. Mech. 46(2): 345-348. doi: 10.1115/1.3424553
19. Rice, J.R. (1988), *Elastic fracture mechanics concepts for interfacial cracks*, J Appl. Mech. 55(1): 98-103. doi: 10.1115/1.3173668
20. Banks-Sills, L., Travitzky, N., Ashkenazi, D. (2000), *Interface fracture properties of a bimaterial ceramic composite*, Mech. Mater. 32: 711-722.
21. Rice, J.R., Suo, Z., Wang, J.-S. (1990), *Mechanics and thermodynamics of brittle interfacial failure in bimaterial systems*, In: Metal Ceramic Interfaces, M. Rühle, A.G. Evans, M.F. Ashby, J.P. Hirth (eds.), Acta-Scripta Metallurgica Proc. Ser. Vol.4, Pergamon Press, New York, 1990, pp.269-294.
22. Deng, X. (1993), *General crack-tip fields for stationary and steadily growing interface cracks in anisotropic bimaterials*, J Appl. Mech. 60(1): 183-196. doi: 10.1115/1.2900743
23. Banks-Sills, L., Ikeda, T. (2011), *Stress intensity factors for interface cracks between orthotropic and monoclinic material*, Int. J Fract. 167: 47-56. doi: 10.1007/s10704-010-9518-1
24. Rice, J.R. (1968), *A path independent integral and the approximate analysis of strain concentration by notches and cracks*, J Appl. Mech. 35(2): 379-386. doi: 10.1115/1.3601206
25. Hutchinson, J.W. (1968), *Singular behaviour at the end of a tensile crack in a hardening material*, J Mech. Phys. Solids, 16(1): 13-31. doi: 10.1016/0022-5096(68)90014-8
26. Rice, J.R., Rosengren, G.F. (1968), *Plane strain deformation near a crack tip in a power-law hardening material*, J Mech. Phys. Solids, 16(1): 1-12. doi: 10.1016/0022-5096(68)90013-6
27. Berković, M. (2004), *Numerical methods in fracture mechanics*, Struct. Integr. and Life 4(2): 63-66.
28. Gurtin, M.E. (1976), *On the path-independent integral for elastodynamics*, Int. J. Fracture, 12: 643-644. doi: 10.1007/BF0034652
29. Sedmak, A., Berković, M., Jarić, J. (1991), *J integral for thin shells*, In: *Defect Assessment in Components - Fundamentals and Applications*, J.G. Blauel, K.H. Schwalbe (eds.),ESIS/EGF9, MEP, London, 1991, pp.45-53.
30. Jarić, J., Sedmak, A., Berković, M. (1988), *On the problem of path dependency of J integral for thin shells*, Proc. 7<sup>th</sup> Europ. Conf. on Fracture (ECF7), Budapest, Hungary, EMAS, 1988.
31. Sedmak, A., Berković, M., Jarić, J., Sedmak, S. (1989), *Finite element method of thin shell J integral evaluation*, Proc. of 7<sup>th</sup> Int. Conf. Fracture (ICF7), K. Salama et al. (ed.), Houston, TX, Pergamon Press, 1989, pp.2111-2117. doi: 10.1016/B978-0-08-034341-9.50216-3
32. Knowles, J.K., Sternberg, E. (1972), *On a class of conservation laws in linearized and finite elastostatics*, Arch. Rational Mech. Anal. 44: 187-211. doi: 10.1007/BF00250778
33. Herrmann, A.G. (1981), *On conservation laws of continuum mechanics*, Int. J Solids Struct. 17(1): 1-8. doi: 10.1016/0020-7683(81)90042-1
34. Bui, H., Jarić, J., Radenković, D., *Loi de Conservation en Thermoélasticité Linéaire*, Ecole Polytechnique, Lab. de Mécanique des Solides, Rapport interne No.3, 1977.
35. Sedmak, S., Sedmak, A., Vukomanović, N. (1990), *Theoretical, numerical and experimental analysis of cracked welded tensile panel*, In: Proc. of 8<sup>th</sup> Europ. Conf. on Fracture (ECF8), 'Fracture Behaviour and Design of Materials and Structures', D. Firrao (ed.), Torino, Italy, EMAS, 1990, pp.1596-1599.
36. Savovic, N., Sedmak, A. (1994), *Numerical simulation of weldment heterogeneity*, Weld. Welded Struct. 39(4): 185-188.
37. Sedmak, A. (1997), *The role of weldment interfaces in fracture mechanics parameters evaluation*, In: Proc. of 9<sup>th</sup> Int. Conf. on Fracture (ICF9), Sydney, Australia, Pergamon Press, 1997, Vol. 5, pp.2345-2356.
38. Smelser, R.E., Gurtin, M.E. (1977), *On the J-integral for bi-material bodies*, Int. J Fract. 13: 382-384. doi: 10.1007/BF00040155
39. Bleackley, M.H., Jones, R.D., Luxmoore, A.R. (1986), *Path dependency of the Rice J integral in weld geometries*, in 'Fracture Control of Engineering Structures', Proc. 6<sup>th</sup> Europ. Conf. on Fracture (ECF6), Amsterdam, The Netherlands, H.C. van Elst, A. Bakker (eds.), EMAS, Vol.I, pp.643-654.
40. Sedmak, A. (2018), *Computational fracture mechanics - an overview from early efforts to recent achievements*, Fatig. Fract. Eng. Mater. Struct. 41(12): 2438-2474. doi: 10.1111/ffe.12912
41. Rice, J.R., Tracey, D.M., *Computational Fracture Mechanics*, in Numerical and Computer Methods in Structural Mechanics (eds. S.J. Fennes et al.), Academic Press, NY, 1973, pp.585-623.
42. Tracey, D.M. (1971), *Finite elements for determination of crack tip elastic stress intensity factors*, Eng. Fract. Mech. 3(3): 255-265. doi: 10.1016/0013-7944(71)90036-1
43. Levy, N., Marcal, P.V., Ostergren, W.J., Rice, J.R. (1971), *Small scale yielding near a crack in plane strain: A finite element analysis*, Int. J Fract. Mech. 7: 143-156. doi: 10.1007/BF0018380
44. McMeeking, R.M., Rice, J.R. (1975), *Finite-element formulations for problems of large elastic-plastic deformation*, Int. J Solids Struct. 11(5): 601-616. doi: 10.1016/0020-7683(75)90033-5
45. Rice, J.R., *Mechanics of Crack Tip Deformation and Extension by Fatigue*, In: Fatigue Crack Propagation, ASTM STP 415, Philadelphia, 1967, pp. 247-311.
46. Read, D.T., *Experimental Method for Direct Evaluation of the J-Contour Integral*, ASTM STP 791, Philadelphia, USA, 1983, pp. II-199-213.
47. Radaković, Z., Abukhres, M., Sedmak, A., Ivanović, I., Petrovski, B. (2013), *Direct measurement of the J integral on a pressure vessel*, Struct. Integr. and Life, 13(3): 163-169.
48. Sedmak, S., Adžiev, T., Gočev, J., Sedmak, A. (1992), *Computerized test for J integral measurement on welded panels*, In: Proc. Int. Conf. on Computerization of Welding Information IV, AWS, Orlando, 1992, p. 161.
49. Petrovski, B., Sedmak, S. (1990), *Evaluation of crack driving force for HAZ of mismatched weldments using direct J integral measurements in tensile panels*, In: Proc. WELDING'90 Technol., Materials, Fracture, M. Kocak (ed.), GKSS Geesthacht, Germany, pp.341-345.
50. Sedmak, S., Petrovski, B. (1988), *Application of direct measurement of J-integral on a pressure vessel with axial notch*, ASTM STP 945, D.T. Read, R.P. Reed (eds.), ASTM Philadelphia, pp. 730-740.
51. Li, F.Z., Shih, C.F., Needleman, A. (1985), *A comparison of methods for calculating energy release rates*, Eng. Fract. Mech. 21(2): 405-421. doi: 10.1016/0013-7944(85)90029-3
52. Banks-Sills, L. (1991), *Application of the finite element method to linear elastic fracture mechanics*, Appl. Mech. Rev. 44(10): 447-461. doi: 10.1115/1.3119488
53. Banks-Sills, L. (2010), *Update - Application of the finite element method to linear elastic fracture mechanics*, Appl. Mech. Rev. 63(2): 020803-1-020803-17. doi: 10.1115/1.4000798
54. Banks-Sills, L., *Interface Fracture and Delaminations in Composite Materials*, Springer Int. Publ., The Netherlands, 2018. doi: 10.1007/978-3-319-60327-8

© 2020 The Author. Structural Integrity and Life, Published by DIVK (The Society for Structural Integrity and Life 'Prof. Dr Stojan Sedmak') (<http://divk.inovacionicentar.rs/ivk/home.html>). This is an open access article distributed under the terms and conditions of the [Creative Commons Attribution-NonCommercial-NoDerivatives 4.0 International License](https://creativecommons.org/licenses/by-nc-nd/4.0/)